


# 2012

Matrix for Chemical IT
(MATCHIT)

Deliverable
Report
D5.4

Grant Agreement No. 249032

**TABLE OF CONTENTS**

# D5.4 Integration of electronic and chemical information processing

## 1 Introduction and objective

The report will demonstrate programmable information chemistry inside the microfluidic-system, showing the process-flow from an algorithm devised in the MATCHIT programming language, using the microstructures to realize the programmed reactions and using the control-software and analytical equipment to verify the coupled synthesis and computation.

The electronically programmable chemical matrix for chemtainer processing was constructed using chemical microprocessor technology involving a microfluidic channel network in two dimensions addressed by a custom high-density gold electrode array on a silicon support. The major thrust of the initiative was to provide a programmable matrix to support the move from molecular chemistry to chemtainer chemistry involving specifically addressed entities. Molecular pathways are based on chemical transport, recognition and reaction, whereas chemtainer pathways are based on chemtainer transport, address matching, reaction, product clean-up and reinjection. An electronically programmable matrix should ideally allow the electronic control of all of these processes, and indeed arrays of electrodes, connected to driving electronics, can provide physical control of all of them. The combination of electrophoretic and electroosmotic effects (both linear and nonlinear) with specific Faradaic (redox) reactions, taking place at electrodes, provides a powerful platform for chemical and chemtainer processing and proved effective in creating an electronically programmable chemical matrix.

### 1.1 Programmable information chemistry in microfluidic system

The information chemistry employed to demonstrate this combination of production and computation uses DNA as an informational molecule, the same molecule used to address the chemtainers, and as the molecules being synthesized. While enzymatic systems (involving proteins) are powerful in DNA processing, most of the microfluidic work in MATCHIT has concentrated on the chemical manipulation of DNA (except for one backup system involving the isothermal nicking strand displacement amplification process, because of its relevance for applications to other projects). The chemical synthesis step utilized in MATCHIT for this deliverable, as a forerunner of more general chemical production, is the ligation reaction attaching DNA oligomers either one to another or to a surface species. The former allows template copying of DNA while the latter allows specific addressing of chemtainer and channel surfaces. Both synthetic steps were primarily pursued using the novel DNA ligation chemistry developed in von Kiedrowski's group at RUB, involving disulphide bond formation. This is a rapid, pH sensitive reaction that had proved productive and generally applicable to both duplex and triplex-based DNA information processing scenarios. The "computations" in the matrix involve specific selection of DNA by timed activation of electrodes and/or electrophoretic separation using orchestrated changes in electrode potentials with optical fluorescent feedback. Chemical activation of electrodes allows the local pH of the solution to be controlled, which in turn switches on and off DNA hybridization in triplexes, and specific surface redox reactions such as disulphide bond immobilization of the activated DNA present in the channel.

### 1.2 Process flow

The basic process flow in MATCHIT is from high level algorithm -> control-software -> microreactor -> coupled synthesis and computation. At the highest level, the MATCHIT calculus (developed at SDU) captures abstract features of the spatially resolved combination of production processes and computation in chemtainer processing, as outlined in Deliverable 6.4. Its focus is on the high level chemtainer objects themselves, and the processing of their contents, and ignores issues associated with timing and physical constraints on the processing. It has been connected with the high level droplet chemtainer processing language (developed at RUB), which handles the spatial location and relocation of chemtainer droplets within the microfluidic topology in addition to their content processing via the

interconnecting gel network. This high level description is mapped (currently with manual support) into the intermediate level scripted language (MATCHIT-IML) which creates programmed sequences of low level chemical microprocessor commands (e.g. at the level of switching voltages on individual electrodes) to direct the chemical matrix microfluidic system. See D6.4 for more details.

# 2 Target reactions for programmable information chemistry

## 2.1 Triplex- and duplex based S-S DNA ligation systems & bead immobilization

The use of (di)sulphide bonds is common in attaching DNA to electrodes, and represents a fundamental synthetic step linking molecular information processing and the production of new structures. Electronic control is achieved via the application of positive voltages to electrodes where specific DNA should be attached and –ve potentials to other electrodes. The starting sequences were immobilized at intermediate surface density for optimal hybridization efficiencies, and the DNA addresses could be relabelled by hybridization to either new single stranded or double stranded sequences. The double stranded sequences allowed the use of pH reversible triplex forming processes, which established a platform for electronically reversible hybridization in the chemical matrix. This platform (initially developed in the ECCell project) was extended in MATCHIT with bulk low voltage pH redox chemistry (quinhydrone system, see 2.2) and with improved hybridization efficiencies and applications to a variety of chemtainer addressing issues (see below). The results were published in conference proceedings and are being integrated into a journal publication.

Von Kiedrowski's group (V. Patzke) has developed a novel rapid ligation chemistry based on disulphide bond formation, which is rapid (timescale of minutes) at moderate temperatures and allows template ligation of DNA with a low background reaction. In joint work with BioMIP at RUB, this reaction has also been extended to DNA triplex interactions, allowing the use of double stranded or hairpin molecules as a template. The pH reversibility of the triplex structure, with the third (Hoogsteen) strand bound at pH 5.5, but not 7.5, coupled with the ability to switch pH in droplet chains and using electrodes, allows a kind of PCR like cycling of ligation and product release without temperature changes. This reaction was chosen as the target for iterative DNA processing in chemtainers (see D5.3).

## 2.2 pH electrochemistry with benzoquinone/hydroquinone redox system

We had developed a procedure to generate on-chip spatial pH changes on microelectrodes for replication chemistry in the ECCell project. The method was extended and optimized in the MATCHIT project to control chemtainer level chemical production and computation processes, moving from an enhanced electrode immobilized redox process to a solution process. The electronic pH regulation is useful not only for thio-replication as well as triple-helix DNA dehybridization but can also be used to change the wettability of properties at the microelectrodes. Furthermore, the method is useful to control processes such as fusion and fission of vesicles and content release (section 2.7) as well as pH induced DNA-addressed bead-bead docking (section 2.8).

### *pH-changes on modified microelectrodes*

Frasconi et al. demonstrated the use of bis-aniline crosslinked Au-nanoparticles for the electrochemical control of the pH of an aqueous solution.[1] In MATCHIT 2-mercaptobenzene-1,4-diol (mercaptobenzoquinone, MBQ) was synthesized[2] and its redox reaction was used for the pH changing process. Microstructures with gold microelectrodes were modified with poly-mercaptobenzoquinone (pMBQ) then the pH changes were monitored using a pH sensitive fluorescent dye SNARF and ratio imaging. Optimized pH cycling results achieved are shown in Fig. 5.4.2.

[1] M. Frasconi, R. Tel-Vered, J. Elbaz and I. Willner, J. Am. Chem. Soc. 132, 2010, 2029–2036.
[2] D. Mascagna, M. d'Ischia, C. Costantini & G. Prota, Synthetic Communications 24(1), 1994, 35-42.

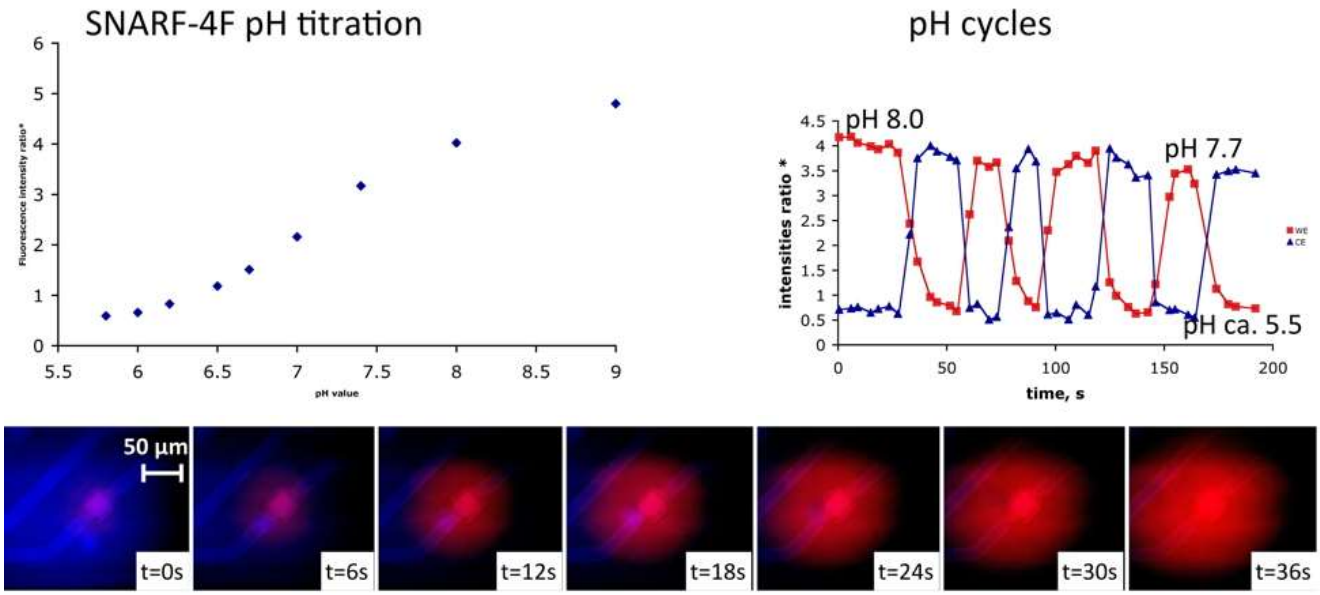


**Figure 5.4.2: pH cycling with electrode immobilized redox system. Left:** The exact pH values were found using titration curve (Sörensen series) in accordance to acquired fluorescence intensity values of $I_{(700)}/I_{(585)}$ by SNARF-4F fluorescence. **Right:** Electrochemical pH changes on microelectrodes detected by SNARF fluorescence. Lower fluorescence image series: Ratiometric image of the pH change on a single microelectrode. Blue colour (positive potential, low pH), red colour (negative potential, high pH).

### *pH-changes in bulk buffer solutions*

The three fluorescence images in figure 5.4.3 shows the pH change actuation in two microfluidic channels (depth 35 µm, width 40 µm) connected with two shallow microchannels (depth 1.5 µm, width 40 µm), involving quinhydrone redox chemistry in the bulk buffer solution.

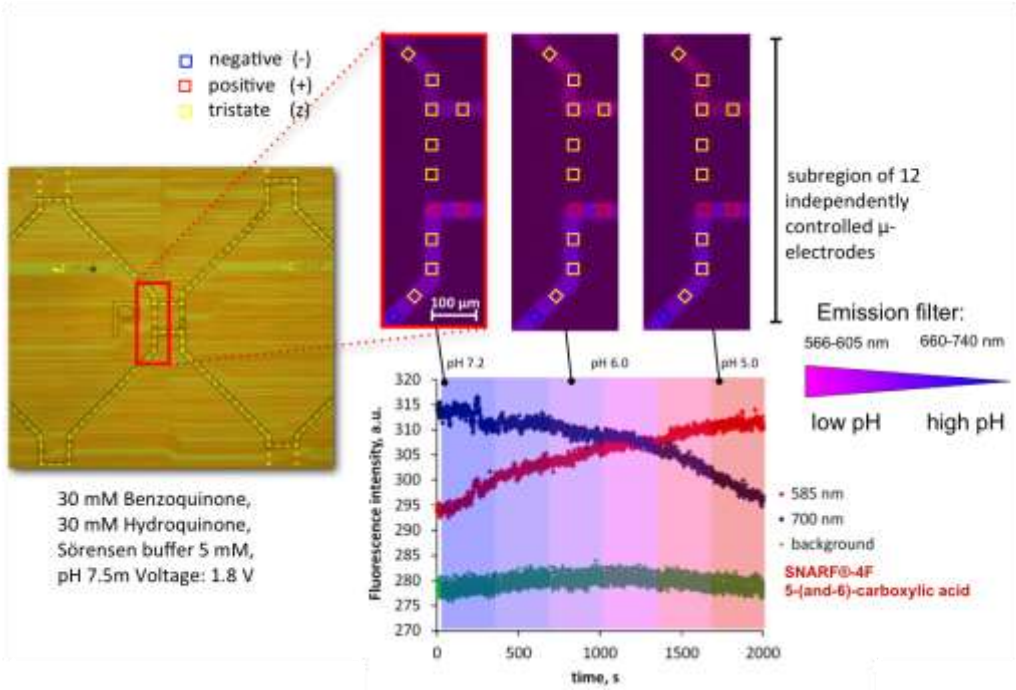


**Figure 5.4.3: Spatial resolved pH environments for Chemtainer processing. (Exposure time: 0.5 s, objective 10-fold, rate of filter switching 0.5 $s^{-1}$) The plots were obtained using the ng_biopro software package. The fluorescence measurement was performed in the upper channel section. pH values were assigned in accordance to initial pH-dependent fluorescence titration.**

### 2.3 Electrochemical activation of gold electrode surfaces

The critical process of sequence specific immobilization of DNA to chosen electrodes in the chemical matrix, undere electronic control, was extensively checked with a comparison between off-chip and on-chip cyclic voltammetry. Special interface PCB cards were developed to allow analog as well as digital control of voltages on the chip electrodes.

For the formation of self-assembled monolayers (SAMs) on gold electrodes we utilized the procedure described in [Anal. Chem. (2000) **72** 2016-2021] in order to activate gold surface electrochemically. The standard Piranha treatment oxidizes any organic material on the surface but also lead to formation of gold oxide, which is not suitable for SAM formation. The electrochemical cell was connected to external Metrohm Autolab electronics and cyclic voltammetry (CV) was performed using GPES software (Figure 1. A). The shift of cathodic peak is exactly the same as shift of anodic peak, which implies possible instability of the potential of the reference electrode.

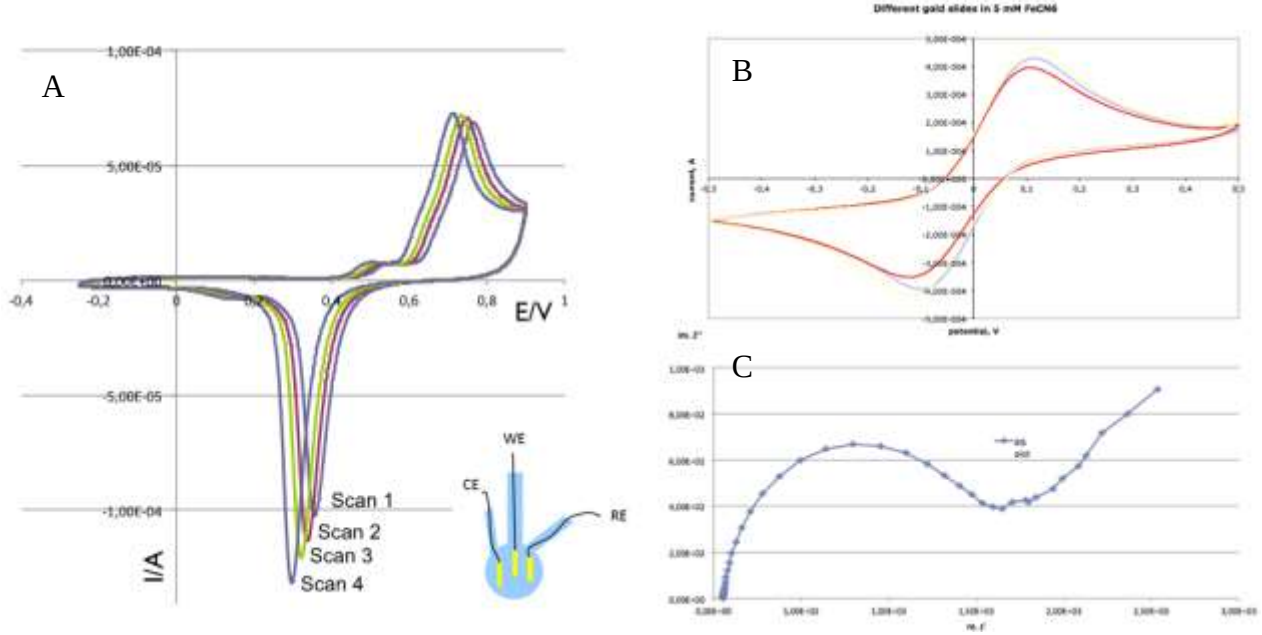


**Figure 1. Electrochemical activation and characterization of naked microscopic gold surfaces.** All experiments performed at three-electrode cell (gold slides 0.5x2.0 $cm^2$). CV curves plotted in coordinates current, A, vs. potential, V. Impeadance measurements are plotted in coordinates ImZ'', Ohm, vs. ReZ', Ohm. A. CV curves obtained in degassed 0.5 M sulfuric acid at 100 mV/s. B. CV curves obtained in 5 mM $[Fe(CN)_6]^{3-}$/$[Fe)CN)_6]^{4-}$ at 100 mV/s. C. Measurements of impeadance in 5 mM $[Fe(CN)_6]^{3-}$/$[Fe)CN)_6]^{4-}$ at formal potential 80 mV as well as at frequency 60 kHz – 0.1 Hz.

The behavior of redox particles such as $[Fe(CN)_6]^{3-}$/$[Fe)CN)_6]^{4-}$ is consistent with activated gold surface giving 200 mV difference between anodic and cathodic peaks on CV curves (Figure 1. B) as well as semicircle of $1.6x10^3$ Ω diameter in impedance measurements corresponded to the electron transfer limited process (Figure 1. C). The immobilization of DNA leads to significant changes of electrochemical properties of gold surfaces in the presence of $[Fe(CN)_6]^{3-}$/$[Fe)CN)_6]^{4-}$ such as increase of the potential difference on CV curve as well as increase of the semicircle diameter in impedance measurements (Figure 2).

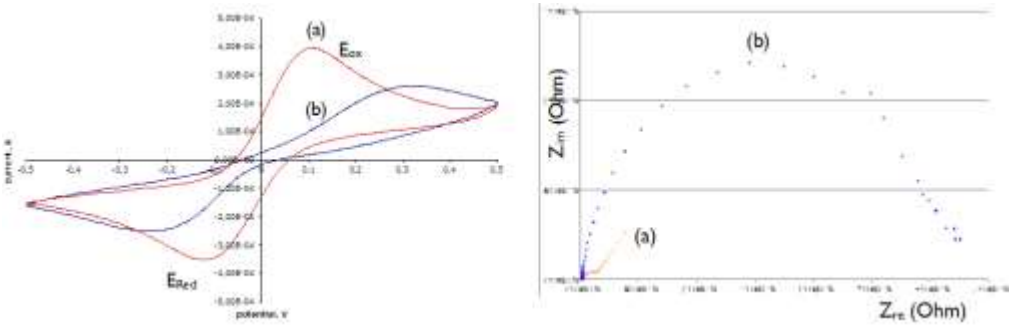


**Figure 2. Electrochemical characterization of microscopic gold surfaces with the SAM of thiolated DNA. Left:** CV curves obtained in 5 mM $[Fe(CN)_6]^{3-}/[Fe)CN)_6]^{4-}$ at 100 mV/s before and after DNA immobilization, following red and blue curve, respectively. **Right:** measurements of impedance in 5 mM $[Fe(CN)_6]^{3-}/[Fe)CN)_6]^{4-}$ at formal potential 80 mV as well as at frequency 60 kHz – 0.1 Hz, performed before DNA immobilization (red curve) as well as afterwards (blue curve).

The microscopic gold surfaces displayed very good performance in electrochemical redox-reactions before any manipulations with the surface. The immobilization of DNA lead to dramatic changes of the electrochemical properties of the surfaces disrupting the redox processes. Similar results were found on the chemical microprocessor chip by connecting gold microelectrodes via external pins to the Autolab system.

### 2.4 Reversible electronic DNA immobilization on microelectrodes

The use of DNA-address-specific manipulation of chemtainer droplets in MATCHIT is only possible at the chemtainer level if we can physically localize droplets for content processing at surface sites (opening to gel processing areas) depending on the DNA labels they contain. Such docking is possible at the molecular level using immobilized DNA complementary to DNA contained in the droplet. Alternative concepts that may be used separately or in conjunction with this are the change of surface wettability of Au electrodes by immobilisation of lipid modified DNA (section 2.5) as well as trapping of droplets via appropriate parking structures or gelation using thermoresponsive hydrogels in microchannels (see also Deliverable D5.3).

We performed first proof-of-principle tests regarding immobilization of thiol-modified DNA on gold electrodes and developed a concept for an electronically programmable immobilization of DNA on microelectrodes: channel segment specific DNA immobilization. Furthermore, we clearly demonstrated both the immobilization and the electrode voltage specific hybridization of DNA to these electrodes. We confirmed the finding of an optimal surface density of DNA for hybridization, and the efficacy of using prehybridized DNA for immobilization to ensure this optical coverage.

We used the following biomolecules for the further development of electronically programmable immobilization of thiol-modified DNA on gold surfaces:

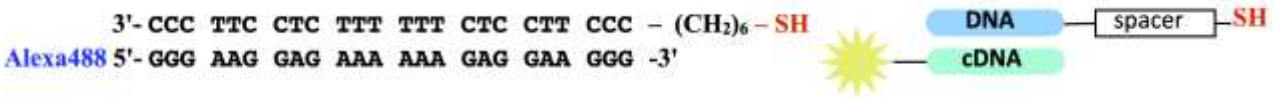


Figure 5.4.4 shows the electronically programmable formation and orientation of stable self-assembled monolayers (SAMs) as well as addressing with microelectrodes: with the final goal to achieve a DNA-addressed location of bead filled droplet chemtainers.

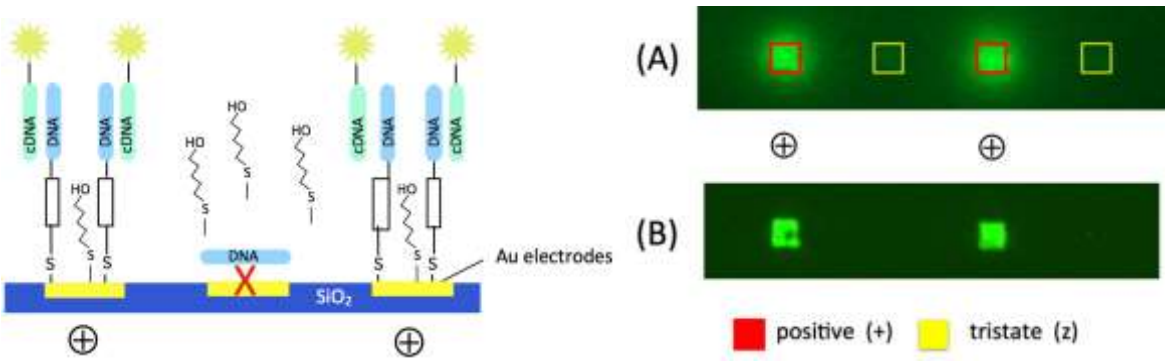


**Figure 5.4.4: Electronically programmable immobilization of DNA in microchannels. (A) Reversible (tracer) concentration & immobilization: 30 min: 1 mM Mercaptohexanol (MCH), 50 mM MES buffer, pH 5.6. (B) Analysis of the immobilized gold surface after washing with in 50 mM His buffer (pH 7.2). No change of fluorescence was observed, when the electrode polarity was inverted.**

Thus effective procedures for the specific covalent loading of electrodes with DNA, so that selective hybridization of specific sequences only to these sites occurs, have been established.

The use of DNA triplex interactions, instead of duplexes, allowed pH reversible DNA hybridization and address relabeling, and completed the electronic programmability of the electrode DNA addressing and readdressing process. Results of this work at RUB-BioMIP are being prepared for publication.

### 2.5 Change of surface wettability with immobilised "lipid" DNA on Au electrodes

Droplet chemtainers are sensitive to changes in the hydrophobicity of channel segments through which they pass. In bypass channel arrangements this can lead to binary differences determining whether or not a droplet parks at a specific location. Making such decisions dependent not only on external signals (such as light or voltage) but upon the interplay of DNA sequences is a core concern in addressable chemtainer processing. One step in this direction, outlined in the activities reported here, involves the use of special amphiphilic modified DNA, see below, hybridizing to the DNA selectively immobilized according to the procedure developed in Section 2.4.

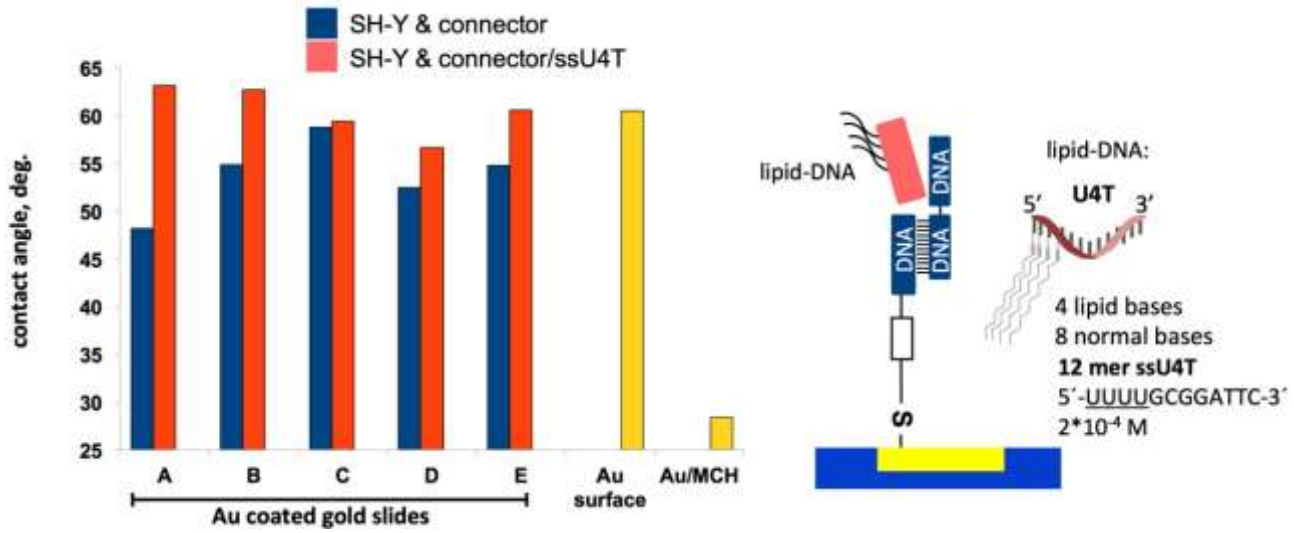


**Figure 5.4.5: Change of hydrophobicity of gold electrodes (left) upon DNA binding (right).**

The specific change of surface hydrophobicity of electrodes is shown by treatment with 6-Mercapto-1-hexanol (MCH) but this is not a DNA sequence dependent procedure. As a step towards sequence dependence that can be linked to the outcome of DNA computations (WP4) we investigated hybridization of lipid DNA ss4UT (A. Herrmann, Rijksuniversiteit Groningen) via a connector strand to our surface bound DNA. A pre-hybridized duplex with single stranded part on one strand as well as

a thiol-group on another strand was immobilized onto the gold surface (Figure 5.4.5, right). This DNA immobilization step leads to decreased contact angles around 50 degrees as shown in the diagram. The single-stranded part serves as the template for hybridization of 12-mer the lipid DNA with four alkyl chains attached to the 5'-end. The following hybridization of the lipid DNA leads to an increasing surface hydrophobicity again.

### 2.6 Sequence-addressed vesicle docking to electrodes

The DNA-directed immobilization of giant unilamellar vesicles (GUVs) on gold electrodes, were performed in a joint collaboration between SDU, RUB (BioMIP) and Weizmann in 2012 and 2013.

The chip surface was pre-treated with thiol-capped DNA, which was attracted to the activated electrodes and immobilized to the microelectrodes surface (RUB). Vesicles with matching or non-matching DNA bound to their membranes (SDU) were transformed to chemical microprocessor chip with and without microfluidic channels. We found that vesicles were highly crowded near positive electrodes and had tendency to stick to the surrounding SiOx surfaces most probably due to hybridization between two DNA strands, one from vesicles and the complementary one sticking non-specifically to whole chip surface. There is a clear difference in the patterns of matching and non-matching populations of vesicles on a chip (Figure 5.4.5a).

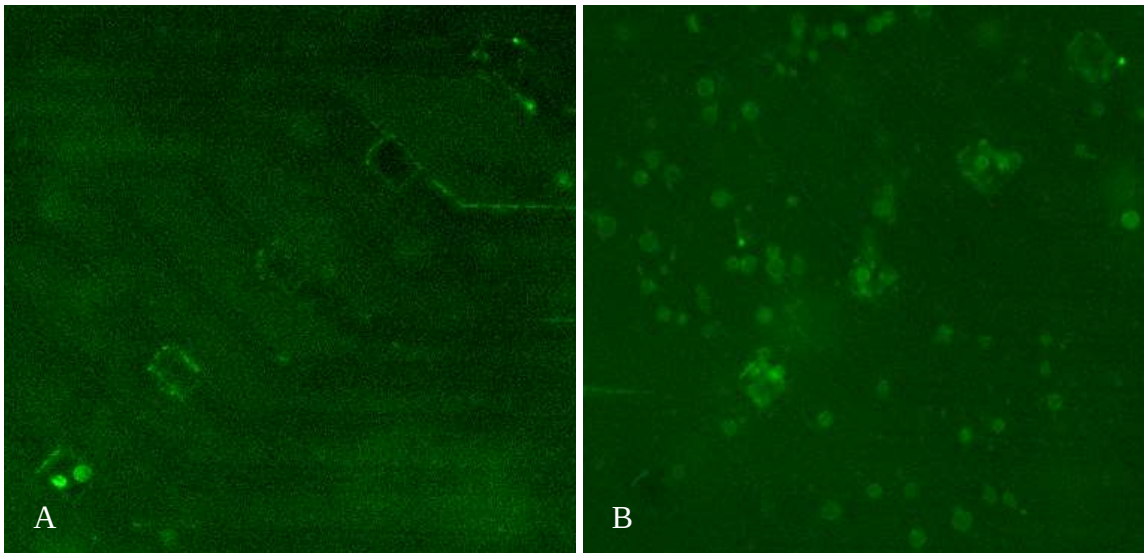


**Figure 5.4.5. Vesicles transformed onto chemical microprocessor without microchannels. A.** Low attachment of vesicles on electrodes with non-matching DNA (nS). **B.** Sequence specific sorting of vesicles on the electrodes with matching DNA (S).

These results were then extended to demonstrate complete DNA addressing of vesicle chemtainers to specific locations in the microfluidic channel network as shown in Fig. 5.4.5b, as documented in a separate manuscript being prepared for publication.

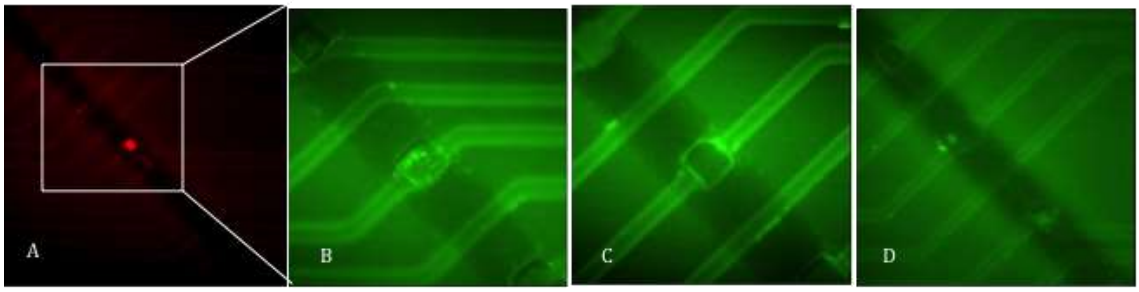


**Figure 5.4.5b. Vesicle chemtainers addressed to matching DNA on electrodes**. A. Combined image acquired at excitation of both, Alexa647 DNA and Alexa488 avidin at 10- and 40-fold magnification, respectively. DNA immobilized to the microelectrode in a microfluidic channel, and vesicles are sorted accordingly to the microelectrodes labeling. C. Vesicles immobilized to the microelectrode via matching DNA (60-fold magnification). D. No vesicles immobilized to the microelectrode (negative control with non-matching DNA immobilized to the microelectrode).

### 2.7 Electronic pH-switched vesicle content release

In a collaboration between SDU and RUB, phospholipid vesicles (GUVs) were converted to reversible chemtainers with a peptide, which is incorporated into the membrane and changes conformation with pH (7.2 to 4-5), thereby modulating the membrane permeability [peptides courtesy of E. Bönzli]. We first established compatibility between these vesicles and the electronically pH switchable hydroquinone system, in order to study impact of electronically driven pH changes on vesicle cargo release. GUVs survived the introduction of 10 mM phosphate buffer, as well as 3 mM quinhydrone system, for electronically driven pH changes. Changes of pH in the range 4 – 7 were assigned with pH-dependent SNARF-4F in former experiments by RUB. We made use of two colour detection of vesicles loaded with DNA cargo in order to follow electronically-driven pH-mediated DNA release from the a membrane. The vesicles were attached to the electrodes by means of sequence specific interactions as in Section 2.6. Separate experiments following vesicles of different sizes in different types of locations were performed: downstream or upstream in the flow, attached close to as well as directly on the electrodes or away from them. Release of cargo upon electronic switching also occurred in the bulk, away from the electrode surface, confirming the pH-mediated permeability of membranes instead of electroporation. In conclusion, vesicles released their content in the presence of switchable peptide which conformation changed upon pH jump (Figure 1). Films document this.

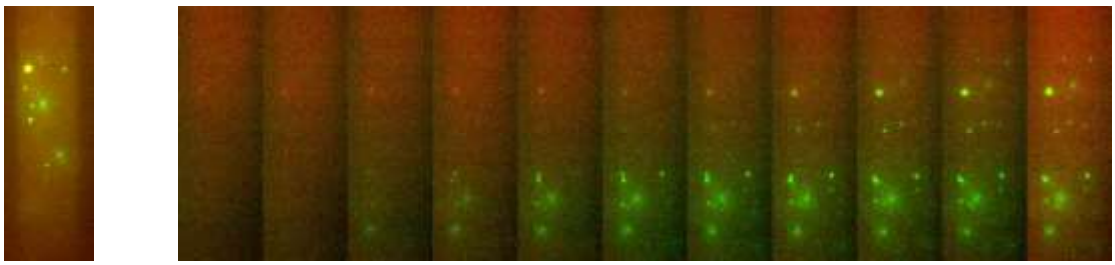

**Figure 5.4.6 Vesicles in microchannel affected by pH. Left**: initial fluorescence of the vesicle at both excitation states, Alexa488 (membrane) as well as Alexa647 (content). **Right**: pH-mediated content release. The fluorescence of both dyes was initially quenched due to the pH pulse and the membrane dye fluorescence was recovered in 11 s (1 s frame interval) the cargo dye was distributed into the surrounding medium.

### 2.8 pH induced DNA-addressed bead-bead docking

This section is less about the properties of magnetic beads, and more about the use of DNA-addressed beads to create DNA addresses from within for droplets. The mechanism employed of DNA addressed bead-bead aggregation is an interesting synthetic process in its own right, adding to the repertoire of electronically controlled information chemical production processes. Before summarizing progress in achieving DNA addressing of droplets using this technique, we briefly summarize the more general role of magnetic beads in the MATCHIT matrix.While magnetic beads cannot be addressed with external magnets at the same resolution as electrodes, without specialized local magnetic coatings,

they do provide an additional level of globally switchable control for DNA processing in microfluidic systems, and they were useful in a number of places in the MATCHIT project (including the iterative processing and vesicle chemtainer addressing process). Magnetic bead processing steps can be introduced into the MATCHIT-calculus with a simple global (or >1mm resolved) on-off switch of the field that arrests and draws together beads where they are in the channel network.

In this section, we demonstrate that specific added DNA, in the form of ssDNA, can give rise to DNA triplex mediated interactions between magnetic beads and cause them to form aggregates (in a pH reversible manner) and these aggregates can give rise to significant changes in viscosity of the solution in which they reside – so that a DNA addressed braking of droplet chemtainers become possible following the injection of a DNA trigger sequence. Since we have established that such sequences can be injected under electronic control, this allows a fundamental solution of the addressing problem for chemtainer droplets: droplets with matching sequences will stop at the braking sites when injected with the appropriate DNA. The initial plan was that this DNA attachment of beads would be to the specific electrodes bearing the appropriate DNA, but the electrode areas currently employed are small for this task. Instead, magnetic beads in the droplets were coated with specific DNA and when a bridging strand was present, the magnetic beads would bind together into a connected network (cf. Figure 5.4.7), which would resist the deformation associated with displacement from the docking site. pH-dependent triplex interactions were used to implement this effect. Such interactions can either be reversed by strand displacement or pH changes (pH5-7).

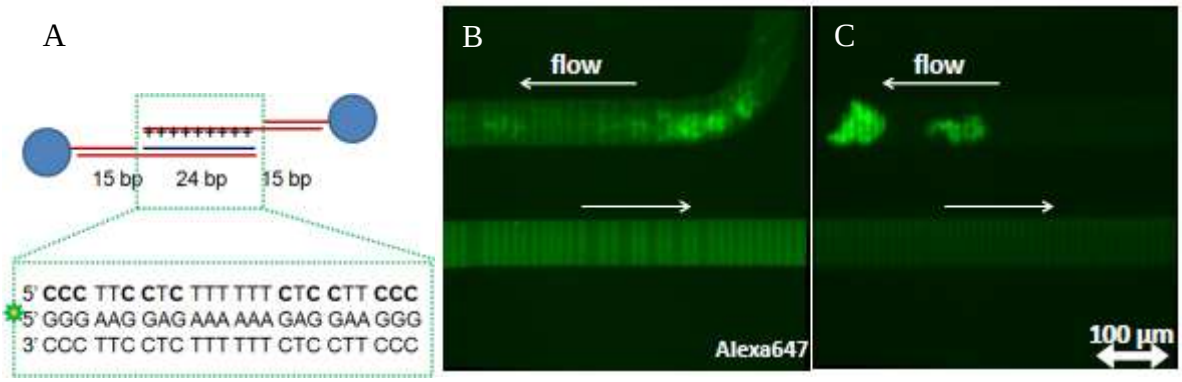


**Figure 5.4.7 DNA templated bridging of beads in a microchannel to brake droplets.** A. Design of DNA construct based on pH-mediated triplex formation. The blue spheres are 1 µm streptavidine super paramagnetic beads. The green sun illustrates Alexa647 dye. B. Online monitoring of formation of bead aggregates in the microchannel using fluorescence microscope. Even in the absence of droplets, beads were braked in the microfluidic turns because of bridging. C. The DNA used to address the bead bridging (and later droplet braking) process was consumed for the formation of bead aggregates in the top channel.

We chose streptavidine super-paramagnetic beads of 1 µm size. In the microfluidic system, those beads are not able to pass 1 µm nozzle in the T-junction. But we can concentrate beads using a magnet at a particular position (1mm resolution) and pass droplets over the retained aggregate of beads. Beads are hydrophilic, they were able to stop air plug moving with flow rate 30 µl/h, though beads were penetrating the surface boundary between water and ionic liquid phases. We investigated pH-mediated bridging of beads via triplex DNA to affect the mobility of droplets in a microfluidic channel.

We annealed the whole DNA construct, containing two double stranded tails, which were bound to the beads via a biotinylated linker (Figure 5.4.7A), at low pH, leading to the formation of pH-dependent Hoogsteen base pairs. The labeled purine strand didn't contain biotin and we proved that DNA doesn't adsorb non-specifically to the beads. The purine strand was mixed with the pyrimidine strand at an equimolar ratio, but all fluorescence was finally attached to the beads and was observed to lead to bead-bead bridging (Figure 5.4.7B). As bead aggregates grew in size, less DNA fluorescence from the linker strand was observed in the channel. Negatively charged beads do not have reason to stick

together and we proved that streptavidine paramagnetic beads without the DNA linker do not form aggregates.

Taking into account that we can switch pH electronically, the bead aggregates bridged via DNA template would contribute to DNA and electronically programmable braking of droplets in a microfluidic channel. Additional material (films) are available to illustrate the mechanistic properties of bead-bead aggregates in microfluidic channels.

## 3. Electronic microreactor design and construction

### 3.1 Design of electronic droplet manipulation (on-demand generation, start-stop, and tracking)

#### *On-chip droplet generation*

Using off-chip droplet generation in microtubes, the choice of carrier fluids, compatibility of ionic (carrier) liquids with vesicles, oil droplets as well as the formation of reverse micelles was reported in the first project period. We found that butylmethylpyrrolidinium bis(trifluoromethylsulfonyl)imide [MeBu][NTF] as well as 1-ethyl-3-methylimidazolium bis(trifluoromethylsulfonyl)imide [EMIM][NTF] (IoLiTec Ionic Liquids Technologies GmbH, Germany) show a good compatibility with PDMS material (used for rapid prototyping of microchannels above the common microelectrode layer) and are successful candidates as carrier fluids regarding droplet formation performance. Several experimental systems were tested to include dye labelled oligomers into aqueous droplets formed in ionic liquids. Tests revealed that labelled DNA does not penetrate the surface boundary to the ionic liquid. Figure 5.4.8 demonstrates the feasibility to control the droplet volumes on chip by regulating the flow rate ratio of the reagent/carrier streams. The image series shows an experiment to control the retention time at the fluid-gel transfer element for a successful product extraction into the separation gel. We can do this by regulating the flow rates of both components: the reagent and carrier fluid as well. The droplet size is increasing by increasing the amount or reagent flow.

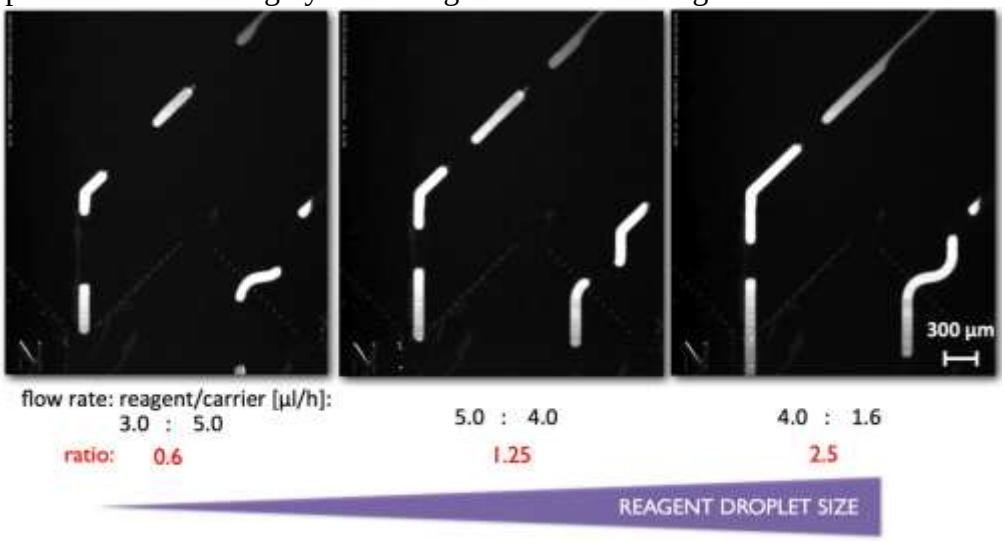


**Figure 5.4.8: On-chip chemtainer droplet generation using ionic liquids** and control of droplet size by regulating the flow rates of both components: the reagent and carrier fluid.

#### *On-demand droplet generation*

The previously achieved programmable droplet size control using normal T-junctions proved insufficient to create the small droplets required for the final objectives of MATCHIT, involving iterative processing and droplet braking. New microfluidic structures were designed, simulated and fabricated at RUB-BioMIP to allow firstly wall-detached and short plug droplets and then more complex droplet sequences such as alternating droplets. One of the successful designs is shown in Fig. 5.4.9. On demand droplet creation, requires precise control of the driving pressures in the fluidic

system. This was achieved using electronically regulated micropumps (Bartel M5, M6) to regulate the exit back pressure to start and stop droplet formation. The control of these micropumps was integrated into the low level control software. The implementation and fluorescence images show an example of alternating droplet chain creation, with the video demonstrating that arbitrary programmable sequences of the two droplet types: not just the alternating ABAB… are possible.

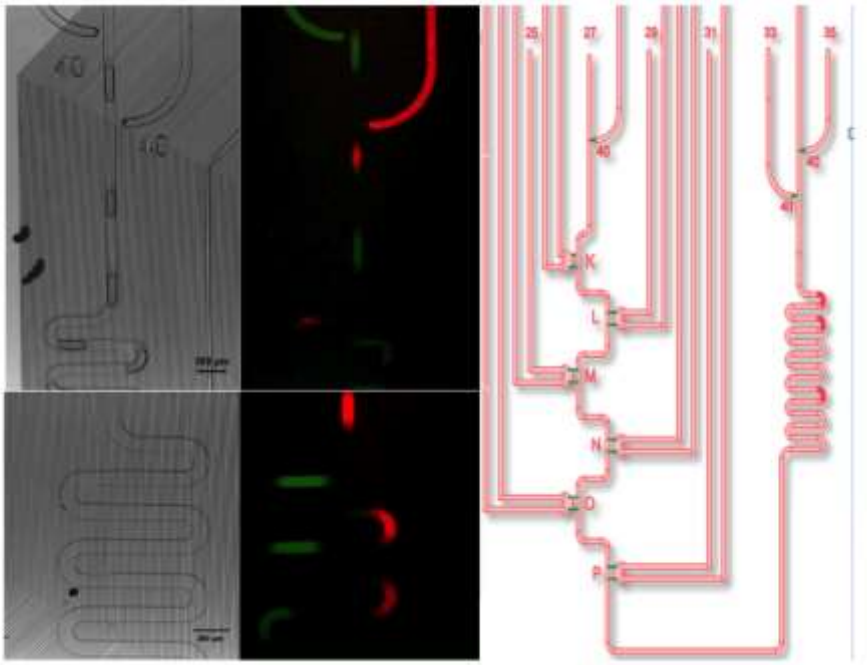

**Figure 5.4.9 Electronically programmable droplet sequences (on demand).** The two inlets 33 and 35 contained green and red fluorescently labelled DNA: Alexa488TCGAGTCTGTTGCAGA CGAATCCGCAAAAGGGAAGGA GAAAA, and Alexa647 CGATGAA-CCTGCGTGA. Droplets were created on demand for these two solutions in the central ionic liquid carrier fluidic channel and propagated downstream in the flow (lower figures). The fine grey lines in the background are insulated wires for the electronic control of downstream processing. (Down-stream structures were used for combinatorial injection in the CADMAD project.)

### *Optical droplet recognition and tracking via rapid image processing*

For image processing we used functions and macros from the free software packages ImageJ (http://imagej.nih.gov/ij) and fiji (http://fiji.sc/wiki/index.php/Fiji).
The workflow of online image processing (see figure 5.4.10) that we developed was:

(1) read in images
(2) build difference images of consecutive images
(3) set threshold (manually) to reduce difference images to 1bit (-> black/white images)
(4a) use function "Analyse particles" to extract position of possible droplets by defining size and shape which results in position and size of object
(4b) using function MTrack2 (http://fiji.sc/wiki/index.php/MTrack2) which uses "Analyse Particles" and additionally tries to track object over the sequence of images.
(5) overlay tracking results with original images

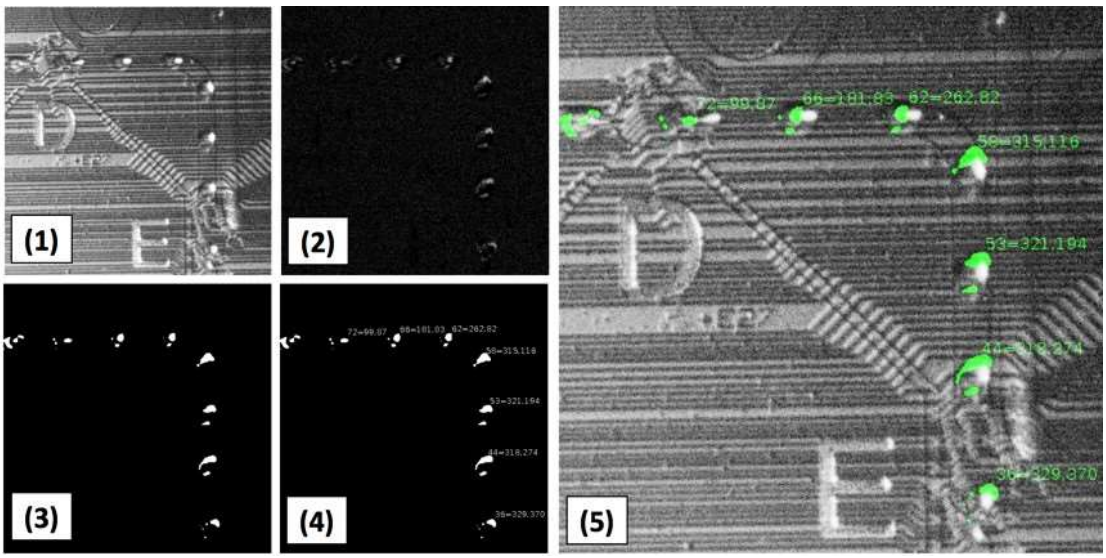


**Figure 5.4.10: Optical droplet recognition and tracking. See text for description of steps.**

This procedure turned out to be rapid enough to allow real-time tracking and labelling of droplets in the microfluidic device. Work is continuing to avoid label interchanges between droplets, to remove the manual optimization of levels for black-white image conversion, and to integrate the software into the overall feedback control system (see also work in WP 6).

### 3.2 Droplet product manipulation: extraction, separation, injection

These core functionalities for electronic chemtainer processing have already been reported in Deliverable 5.2.They will also be utilized in part in the iterative processing Deliverable 5.3 demonstration. These processes were optimized in MATCHIT in the final year, using simplified microfluidic structures as shown in Section 3.4 and the revised D5.2. The overall process of reaction and product cleanup from one droplet to another, which involves these three processes, will serve as the core example of the programming flow targeted by the deliverable in Section 5.

### 3.3 Overall MATCHIT matrix for chemical IT

In MATCHIT, we designed and built a fully integrated electronic microfluidic matrix for the integration of production and computation, as reported in year two. The basic concept was extended from the proposal, to allow continuously flowing resource channels to deliver fresh chemicals and extract waste from droplets, via artificial membranes in the form of shallow ledges under electronic control as shown in fig. 5.3.10. The design also allows varying degree of separation through branching points in the separation matrix, and through the systematic use of hydrodynamic barriers and reversibly gelled separation media (custom pluronics mixtures) both upstream and downstream product transfer in the chemtainer droplet chain. The figure shows successive chemtainer droplets moving along the meandering daisy chain channel under white light. Droplets can be moved through the matrix as well, material can be exchanged with the environment, and the information content of droplets (e.g. current set of DNA molecules) can be extracted and processed in the gel network matrix. Although the IO structure of this implementation of the MATCHIT matrix is somewhat asymmetric and complex, to allow buffered resources to be supplied at specific local sites, the matrix itself is regular. In year 3 of the project, we returned to the more simple droplet chain processors, initially envisaged, without buffered resources.

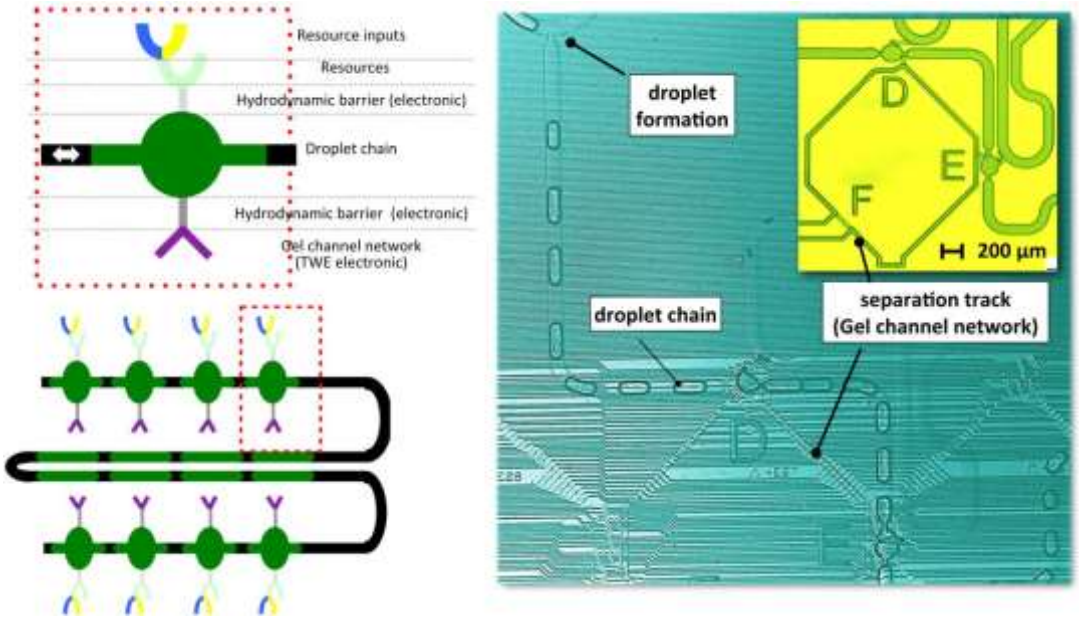


**Figure 5.3.10: The left scheme shows a schematic view of the basic network module of the electronically programmable chemical matrix involving a fast serial droplet track (green/black) and slow (grey/violet) gel based reaction processing tracks. The right large microscope image illustrates the complete assembled PDMS microfluidics with electronic layer with droplet flow inside. The small yellow image shows the SU8 master structure for PDMS rapid prototyping. The resource channels are shown in the upper right corner of the image and the inset.**

The overall design for microfluidic integration to do a complete cycle of droplet reaction, extraction to gel, product separation in gel as well as the reinjection of bands to a container droplet is shown in figure 5.3.11. The droplet meander crosses the chip four times horizontally and material can be processed to both upstream or down stream droplets. In this design, extraction and reinjection is possible at 8 dedicated sites (A-H).

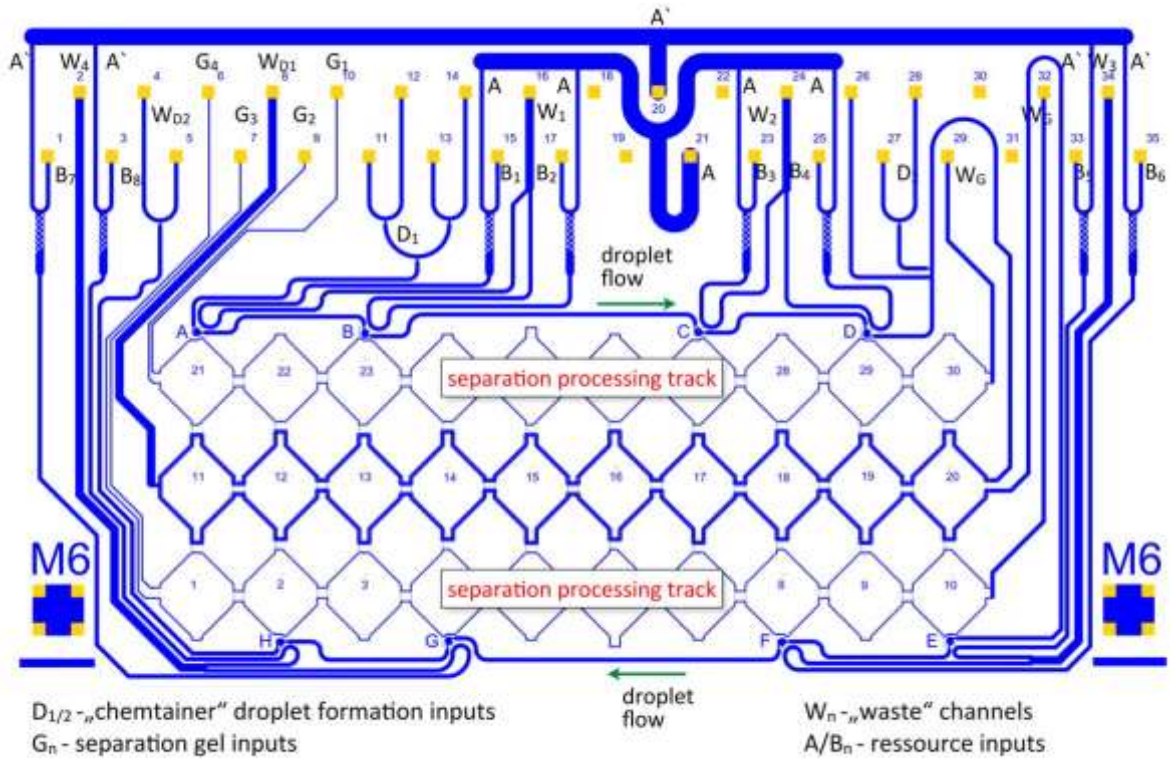


**Figure 5.3.11: Full microdroplet processor design** (electrode arrays following the channels not shown). Droplets are generated at inputs D1 (11-14) and flow from left to right across the top (past the sites A,B,C,D) and then back and forth through the center and finally from right to left (past sites E, F, G, H). Individual resources with on chip mixers flow by the

8 sites A-H allowing resource replenishment across the hydrodynamic barrier ledges. Gel separation structures allow parallel electronic content processing between different droplets.

### 3.4 Simplified microfluidics for DNA processing

The separate microfluidic functions required for droplet processing were investigated intensively in the final year of the project. In particular, multiple iterations of droplet braking structures were performed in conjuction with simulation. The successful parking of droplets at sites for electronic processing is shown in Fig. 5.3.12, and is documented by extensive video material.

To optimize the microfluidic designs we performed Computational Fluid Dynamics (CFD) simulations using the open source solver OpenFoam (http://www.openfoam.com/). We studied the performance of designs by varying the boundary conditions and parameters such as flow rates and pressure. The properties of different fluids were introduced by defining transport properties such as densities, contact angles, and viscosities. Fluid flow was assumed laminar without turbulence at the low Reynolds numbers employed. We studied the performance of designs for T-Junctions for droplet formation, droplet oscillator models to study collective droplet motion, and droplet parking junctions. Examples of CFD simulations are shown in Fig. 5.3.13. Starting with solutions taken from the literature, designs were modified and optimized through the simulations (A. Sharma, RUB-BioMIP). One of the several droplet processing design iterations for microfluidic fabrication is shown in Fig. 5.3.14.

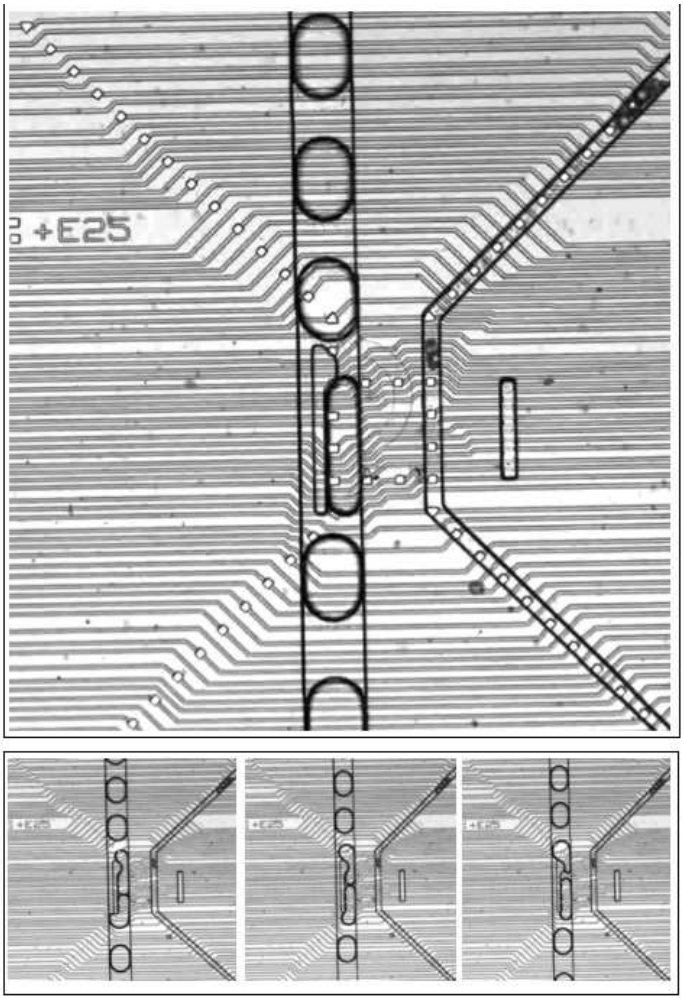


**Figure 5.3.12 Droplet braking at defined locations for content processing. Bottom:** 3 successive images showing braked droplet displacement and release in Pluronics stabilized droplets. **Top:** Close up of droplet braking at bypass structure in 100µm channel (left), with narrower gel channel for content processing (right), and shallow (1µm) hydrodynamic barrier connections (centre).

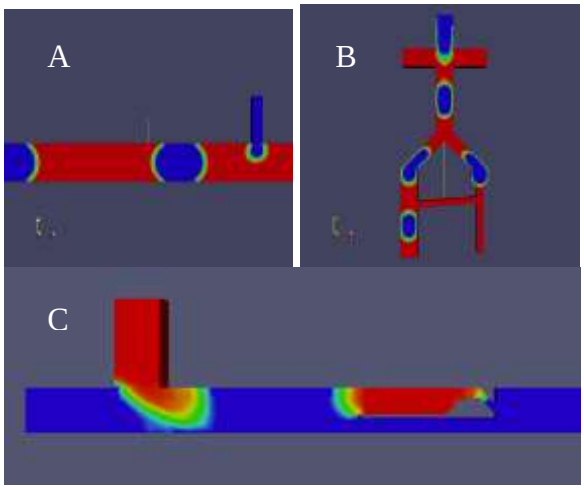


**Figure 5.3.13: Simplified microfluidics for droplet processing: CFD simulations.** A: Droplet formation at narrow T-Junction B: Droplet oscillator, showing parked droplet on the right side. C: Droplet parking structure. Various parts of microfludic structures were designed and meshed using **Salome** (**http://www.salome-platform.org/**). The Volume Of

Fluid (VOF) method was used with a stationary mesh, as it allows one to track the shape and position of the interface. Two solvers, InterFoam and MultiphaseInterFoam**,** were used for the two phase and multiphase fluidic systems.

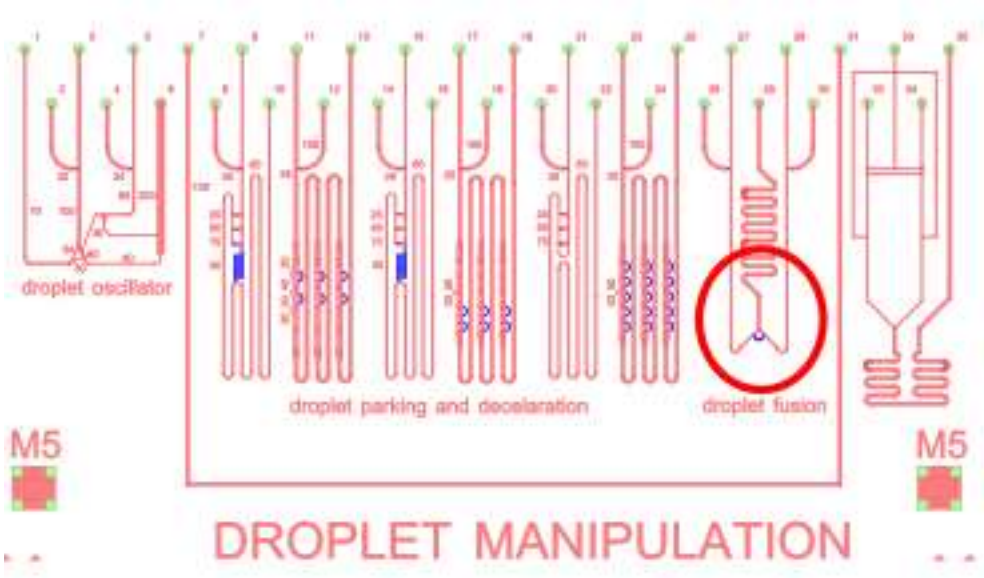


**Figure 5.3.14: One of the simplified droplet processing test chip designs.** Droplet parking structures are microscopic but can be seen in Fig. 5.3.12. The blue channels are pressure equalization channels used to stabilize the hydrodynamic designs.

## 4. Electronic microfluidic control system and MATCHIT programming language

Details of the electronic microfluidic control system and MATCHIT programming language are provided in Deliverable 6.4 and elsewhere in the MATCHIT reporting, so that we do not repeat this documentation here. We show the overall structure of the language relationships again for reference:

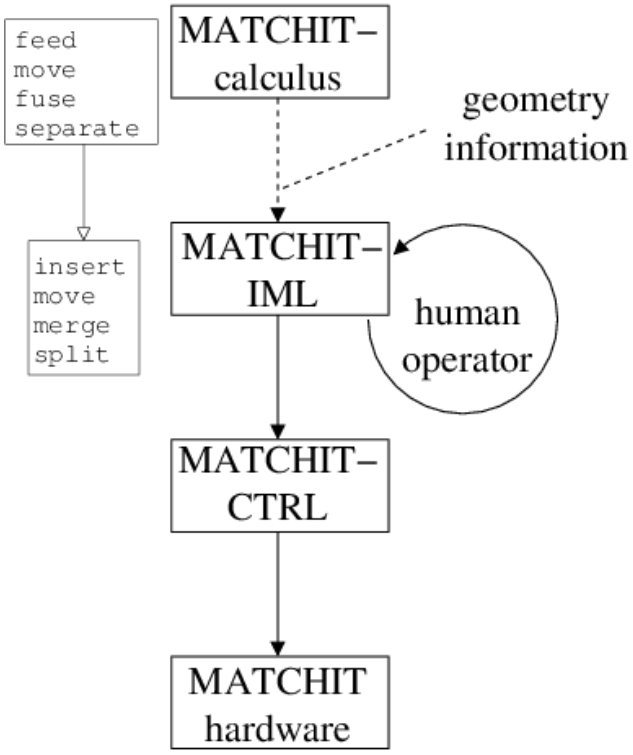


**Figure 5.3.15: Workflow to create MATCHIT hardware machine code from programs generated by the MATCHIT calculus from D6.4.** The MATCHIT compiler generates a solution to the given synthesis problem only requiring the user to write a set of the three types of chemical rules (canonical form, classifiers and basic operations). The compiler would then write out an intermediate script of low-level commands, which can be edited by the human operator. This script of low-level commands will then be translated by an assembler stage, which produces a script with all the detailed instructions to solve the high-level specified problem, see the ng_biopro-user-manual as a reference for available commands and available operations.

The MATCHIT hardware referred to in this diagram includes the chemical microprocessor chips, electronic adaptor boards, syringe and membrane micropumps, electronic regulated laser system (incl. AOTF color switching and custom galvanic line scanning system), motorized microscope, CCD based optical imaging system, temperature control system, translation stages for samples and magnets, external computer hardware.

## 5. Integration of electronically controlled chemistry and computation

The objective of this section is to demonstrate the operation of certain constructs of the MATCHIT-IML (InterMediate Language) in the experiments. This MATCHIT-IML has been specified in the deliverable D6.4 and earlier activity-reports. Only a subset of the operations specified in this language is shown in the following. There are basic chemtainer operations in the IML such as:

- loop V, which executes rule V *k* times.
- halt the execution of the system.
- wait, for a specific amount of time, at a specified temperature.
- mixture, a recipe to combine chemicals or nano-containers in a chemtainer.
- merge, *n* chemtainers are merged into a larger chemtainer, c.f. fuse()-operation in the calculus.
- select, a chemtainer from *k* chemtainers.
- sequence, process chemicals in a sequential manner.
- start and stop a specific chemtainer-chain.
- target, the chemical which should be delivered in an output-chemtainer.
- separate a specific (length) sequence from the rest of the mix.
- create a new droplet

These are supported by low-level operations:

- Start and stop of a chemtainer-chain, whether they are from the input-set or one of the many possible registers, they must be stoppable individually, see movie [sibelius:8168/ng_biopro_vid_20130327_1657xxx_elec.mp4] or movie [sibelius:8168/ng_biopro_vid_20130327_1702xxx_elec.mp4] which demonstrates stopping the

chemtainer-chain for more than 25 minutes.

- Insert material into a chemtainer. The material must be affected by electric fields and it will be extracted from the gel-phase in the transportation and separation network, see example in figure 5.
- Extract material from a chemtainer. The material must be affected by electric fields and it will be inserted into the gel-phase in the transportation and separation network, see examples in figure 6 and 7.
- Transport material along the transportation and separation network, if this material is sensitive to electric fields, see Listings 1-3.

The integrated process topology is depicted in Figure 5.3.16, which shows two separation lanes coupled with two chemtainer channels such that an iterative processing of the chemicals inside the chemtainers can be realized. Chemtainers flowing in channels undergo reactions induced by content injection (or fusion) and the reaction products are extracted, separated and reinjected in new chemtainers to allow ongoing iterative processing.

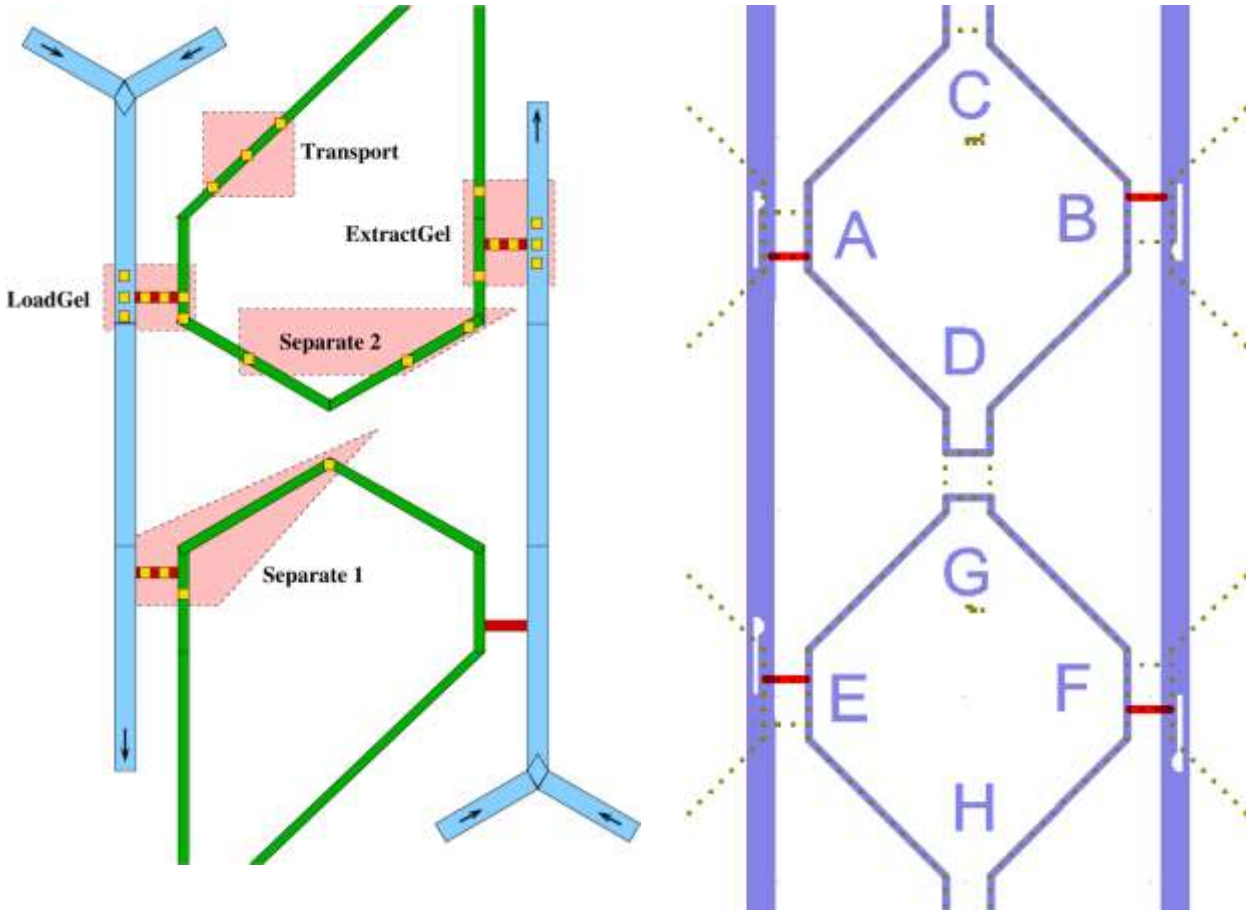


**Figure 5.3.16: Simplified MATCHIT chemtainer processing architecture & realization.** Two separation lanes are connecting two chemtainer channels which can be individually controlled. The chemtainer flow in the left is from top to bottom and opposite in the right channel. Via the small red-drawn EOF-barriers (electro-osmotic flow) charged material can be extracted from a chemtainer and be e.g. cleaned in the separation channels and reinserted into a new chemtainer with new resources to be processed further. The topology allows for an iterative processing. On the right hand side of the figure the real microfluidic design is shown. The small inlet in the chemtainer-channels are the droplet-braking barriers.

A MATCHIT-IML program is shown in the section on Listing 4, which makes clear the connection to the abstract MATCHIT-calculus.

## Separation

Separation of DNA-oligonucleotides proved a continuing challenge using low voltage arrays of electrodes. The successful simulations of TWE-based separation (Travelling Wave Electrophoresis), see EU-project ECCELL, proved to be difficult in microfluidic structures, because of field inhomogeneities and local chemical reactions in our microfluidic structures, despite the extension to feedback wave electrophoresis (with content sensing dependent switching of electrodes, via fluorescence feedback). Extensive work on enhancing separation was performed in both the MATCHIT and CADMAD projects, for the different project goals. Avoiding local interactions by making use of distant electrodes, proved not possible because of diminishing field strengths and separation times were too long to be practicable. With a new PCB, see Figure 5.4.17, arbitrary voltages in the range of 0V to 15V can be applied under computer control to all of the available electrodes. Voltages above 10V yield strong artefacts (beyond the known and well simulated nonlinear effects above the thermal voltage, 25mV) in the microfluidic channels. All experiments shown in the sequel have been done at a maximum potential of +9V with the separating electrodes having a distance of 1-2 mm, which gives field strengths of 40 to 80 V/cm.

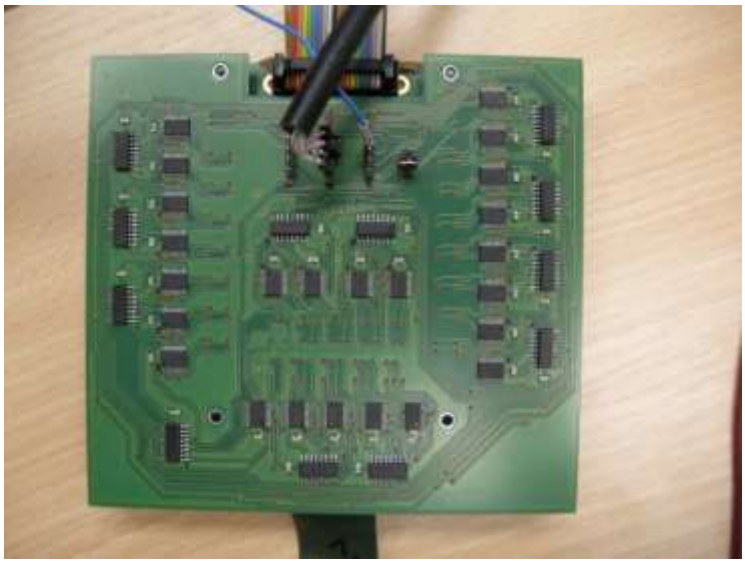

**Figure 5.4.17:** A "high-voltage" driving printed circuit board allowing up to 15V of potential to all of the available electrodes asserted. [RUB-BioMIP 2011-2012]

With these high field strengths and electrodes, at least 1mm apart, separation could be successfully established. See Figures 5.4.18 and 19 for demonstration of separation. The times given represent the time after starting extraction of material from the resource channel. The extraction itself will be shown below. In the separation an effect is already visible which turned out to occur for all separation experiments done so far. After the separation of the two DNA-oligos they suddenly were drawn by strong forces to a fixed virtual point in the separation channel staying there put until the hydro-gel was melted again for cleaning purposes. Due to this location being an extremely small region all DNA became so highly concentrated that quenching occurred and the fluorescence signal vanished.

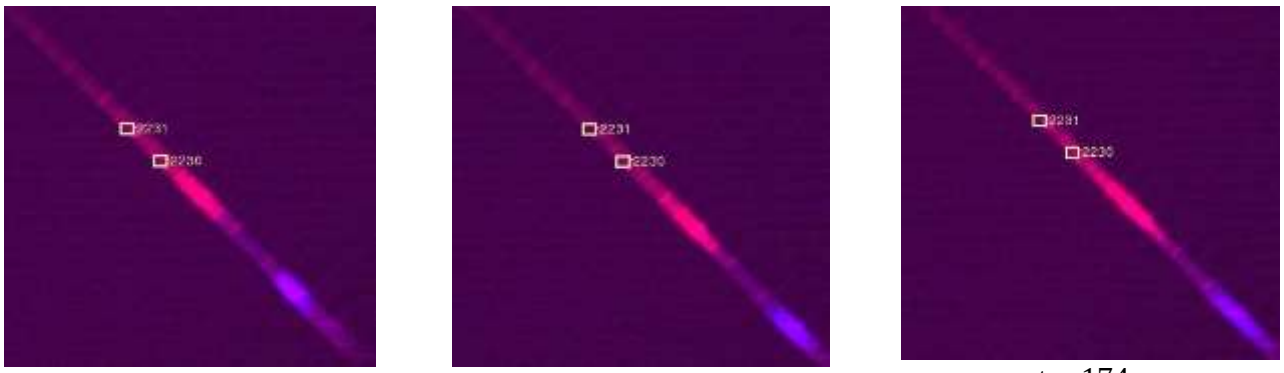


t = 85s t = 106s t = 174s

**Figure 5.4.18: DNA separation in the gel network.** 50mM His pH7 + OligoN2b(24nt, Alexa488) 2*10e-7M and OligoAlphaY1(45nt, Alexa647) 2*10e-7M, adding urea was possible when staying below 2M (0.1M, 1M and 2M urea proved working, 7M not) of concentration.

This behaviour has been observed over many tens of experiments and shall be illustrated at one further example, shown in Figure 5.4.19. The dynamics of the separation can be easily seen. While this is most likely the result of space charge depletion effects, and these are exaggerated by the low ionic strength of the solutions used, the non-linear DNA movement is not yet fully quantified and may also involve structural deformation of the cross-linked micellar gel matrix (Pluronics).

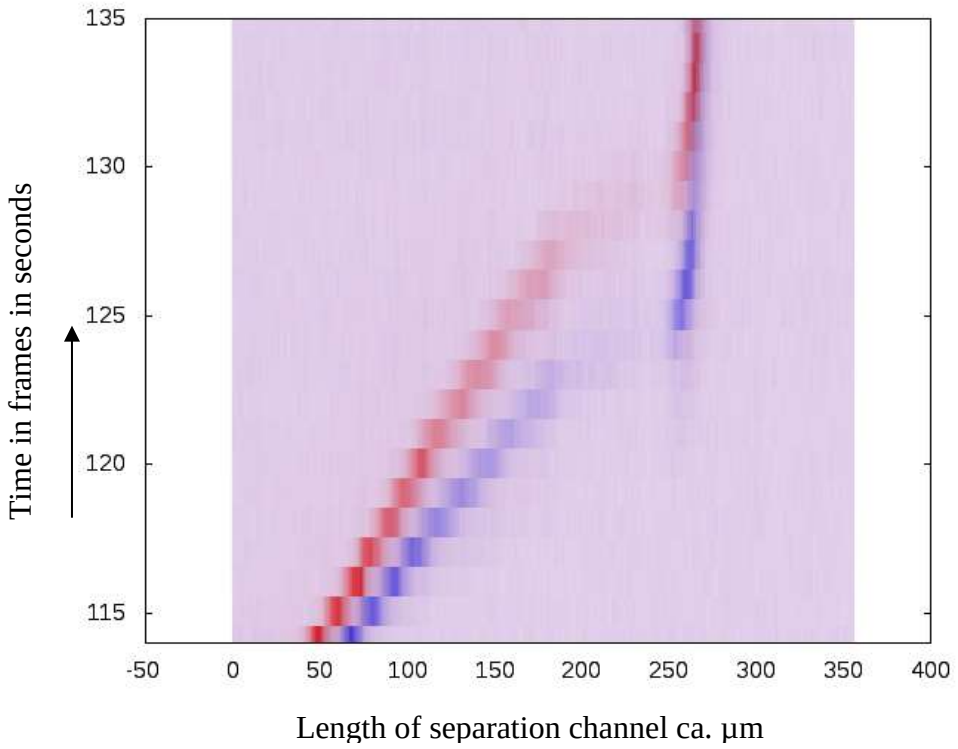


**Figure 5.4.19: Density plot of separation of DNA at strong fields, showing limited window for separation.**
The input channel is filled with 50mM His pH7 + OligoN2b(24nt, Alexa488) 1*10e-7M and OligoAlphaY1(45nt, Alexa647) 1*10e-7M, while the gel channel is filled with 30% F87 Pluronic in 50mM His pH7. The image is a space-time-density plot of the resulting separation, with red representing the long 45nt oligo and blue the short 24nt oligo. The extraction is not shown and shortly after separation began, the picture shows the behaviour along the channel (x-axis) over time (y-axis). At frame 125 and location 180 a sufficient separation is visible. The oligos then move with high velocity to the collection point, about 80% of the interval. After 135 s the fluorescence is quenched.

Similar behaviour could also be observed in low melting point agarose gels, although the gel-matrix not being fine grained enough to be able to separate the two DNA strands, data not shown. What role the buffer solution plays in this scenario is not yet known, HIS buffers gave the best results for separation. Tris acetate buffer and other commonly used buffers in enzyme systems showed poor results (data not shown). Other reversible gel-matrices were also employed.

## Transport

An even more fundamental processing operation to implementing the MATCHIT calculus is the transport of material under electronic control, and we will illustrate the different levels of software control in more detail using this example. Transport of material along the transportation and separation network is possible, if this material is sensitive to electric fields. To simplify the software architecture the two-dimensional transportation grid is mapped into an essentially one-dimensional system with only channels available. These channels are anchored at the available electrodes. In addition, around the electrodes areas are defined which averaged fluorescence intensities are interpreted as values from virtual sensors. In Figure 5.4.20 such an example is shown: the channel is not visible in this fluorescent image, where a cluster of a mixture of DNA-oligos is moved via electrical forces in a Pluronic gel-matrix back and forth.

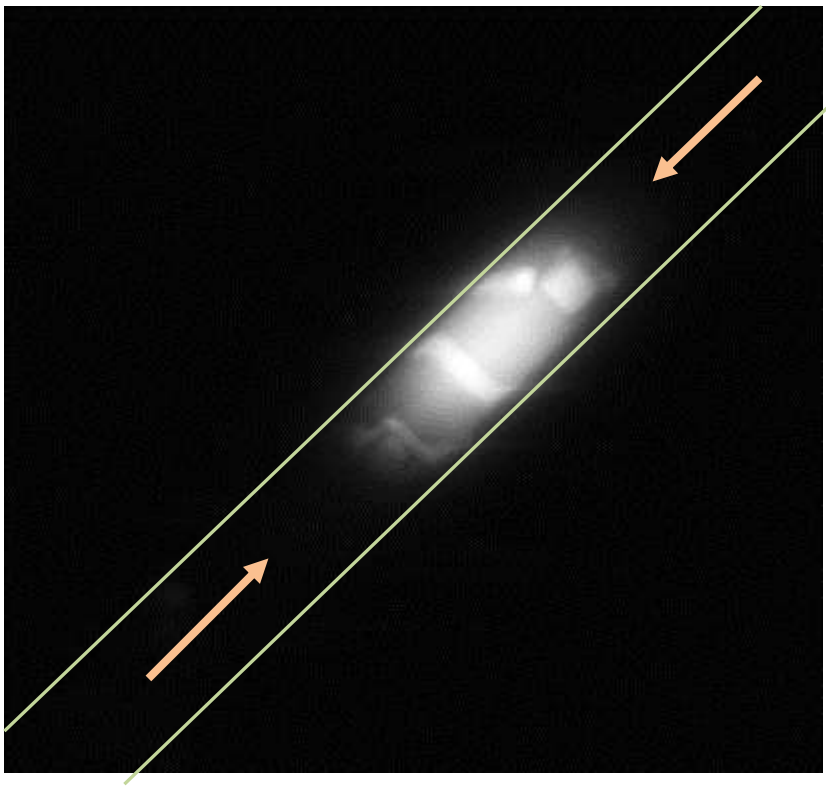

**Figure 5.4.20: Transport of DNA autonomously under electrode control.** Moving this cluster along the channel autonomously with spatially distributed feedback controllers, depicted in Listings 1 and 2, see movie [http://fp7-matchit.eu/admin/upload/Deliverables/Final-Report]. The experimental details are: Module W367291210, channels 28 and 29 (blocked) are filled with 25% Pluronic(127:87;2:1) in His 50mM pH7,2 +Oligo N (24mer)1e-7 M Alexa 647 +Oligo 4 (30mer) 5e-7M Dy481XL and channels 30,31,34,35 are filled with $H_2O$.

This transportation is realized with several feedback-controllers, see Listing 2, which are distributed along the channel. As mentioned above, the electrodes in the channel are used as the anchor-points for the feedback-controllers. A single feedback controller can be seen in Listing 1. This feedback-controller essentially is a free-form state-machine which state is triggered by the surpassing of thresholds at the according virtual sensors around the electrodes. All eleven feedback-controllers are arranged such that each controller reaching its final state triggers the next controller. Five controllers are used to move the cluster forward and another six of them to move the cluster backwards again. These controllers are connected in a ring like fashion. In the experiment shown, the cluster could be moved at least three times back and forth before fluorescence started to decrease due to bleaching and losses of material.

```
control_group $1 0 $2
control_group $1 1 $6
control_group $1 2 $4
control_sensor $1 $3 $4 $5 $6
control_reference $1 $2 $3 $4
set_sensor $1 sen_$2 high_thr 2.8
set_sensor $1 sen_$3 high_thr 2.80
set_sensor $1 sen_$4 high_thr 2.80
set_sensor $1 sen_$5 high_thr 2.80
set_sensor $1 sen_$6 high_thr 2.80
nr_states $1 4
#                                  0->1 event=1, 1->0 event=0
#        name state sensor   ev pri tout nst nh {list} nl {list} nt {list}
add_state $1   0   sen_$4     1  5  100   1   1   1    1    0     0
add_state $1   1   sen_$5     1  5    0   2   0        0          0
add_state $1   2   sen_$6     1  5    0   3   0        0          2   0 1
add_state $1   3    $7        1  5    0  9997 0        0          0
```

**Listing 1:** A feedback controller is shown trying to move a cluster of material from location A to location B.

```
eval_channel design/fluidic/biopro61_std/M3_B5_SEG.dat

control_add autoshift1 "general" r713
control_add autoshift2 "general" r712
control_add autoshift3 "general" r711
control_add autoshift4 "general" r710
control_add autoshift5 "general" r709
control_add autoshift6 "general" r704
control_add autoshift7 "general" r705
control_add autoshift8 "general" r706
control_add autoshift9 "general" r707
control_add autoshift10 "general" r708
control_add autoshift11 "general" r709

#set_pin r1618 low   # Shielding with negative electrodes
#set_pin r718 low    # Shielding with negative electrodes
auto_shift_4 autoshift1 r713 r712 r711 r710 r709 autoshift2
auto_shift_4 autoshift2 r712 r711 r710 r709 r708 autoshift3
auto_shift_4 autoshift3 r711 r710 r709 r708 r707 autoshift4
auto_shift_4 autoshift4 r710 r709 r708 r707 r706 autoshift5
auto_shift_4 autoshift5 r709 r708 r707 r706 r705 autoshift6
auto_shift_4 autoshift6 r704 r705 r706 r707 r708 autoshift7
auto_shift_4 autoshift7 r705 r706 r707 r708 r709 autoshift8
auto_shift_4 autoshift8 r706 r707 r708 r709 r710 autoshift9
auto_shift_4 autoshift9 r707 r708 r709 r710 r711 autoshift10
auto_shift_4 autoshift10 r708 r709 r710 r711 r712 autoshift1
```

**Listing 2:** Moving a cluster of DNA molecules back and forth in a channel in an autonomously feedback controlled manner. The command 'auto_shift_4' which is called from this script is depicted in Listing 1.

Instead of using a fixed set of distributed feedback-controllers a single moving feedback-controller can be realized. As an example of that, a slightly higher-level programming listing is shown in Listing 3, which shows the code to move an electrode pattern along the given path 'slider'. This example uses the concept of an instance, which is the logical construct of a chemtainer. It also shows how parallel and sequential programs can be developed in the system, which are derived from the MATCHIT-IML and the compiler, which finally is fed by the MATCHIT-calculus.

This language level uses the concept of a 'task' with all tasks executed in parallel and the code inside a task executed sequentially. Due to the physics of the hardware, it is necessary to allow for sequential operations because the field-of-view of the camera can only capture a small part of the whole story and as such the microfluidic chip must be moved with a XY-table towards the regions-of-interest.

```
eval_channel biopro61_oct11/M34_B5_SEG.dat
instance test_inst_a
pattern pat_a 16 # A membrane of 16 elements.
addprop pat_a graphic Microscope
addprop pat_a electrode r1835
addprop pat_a pattern 0 2 2 1 2 # Middle electrode is active.
addprop pat_a area 40
addprop test_inst_a pat_a

task t1
path slider r1768 r1816
exec set_pin r1767 low
exec set_pin r1772 low
exec set_pin r1808 low
exec set_pin r1814 low
exec set_pin r1815 low

exec assign ctr 0
do
    exec echo increment $ctr
    move test_inst_a slider $ctr
    exec incr ctr
    if iseq $ctr 2000
        break
    endif
    exec sleep 14
enddo
endtask t1
```

**Listing 3:** This script shows the concept of a controller moving. The controller in this case is a pattern which is dragged along a given path ('slider' with the boundary electrodes 'r1768' and 'r1816').

The script-language is descriptive and executable in the same instance. In cases where there can be conflicts the command 'exec' is used.

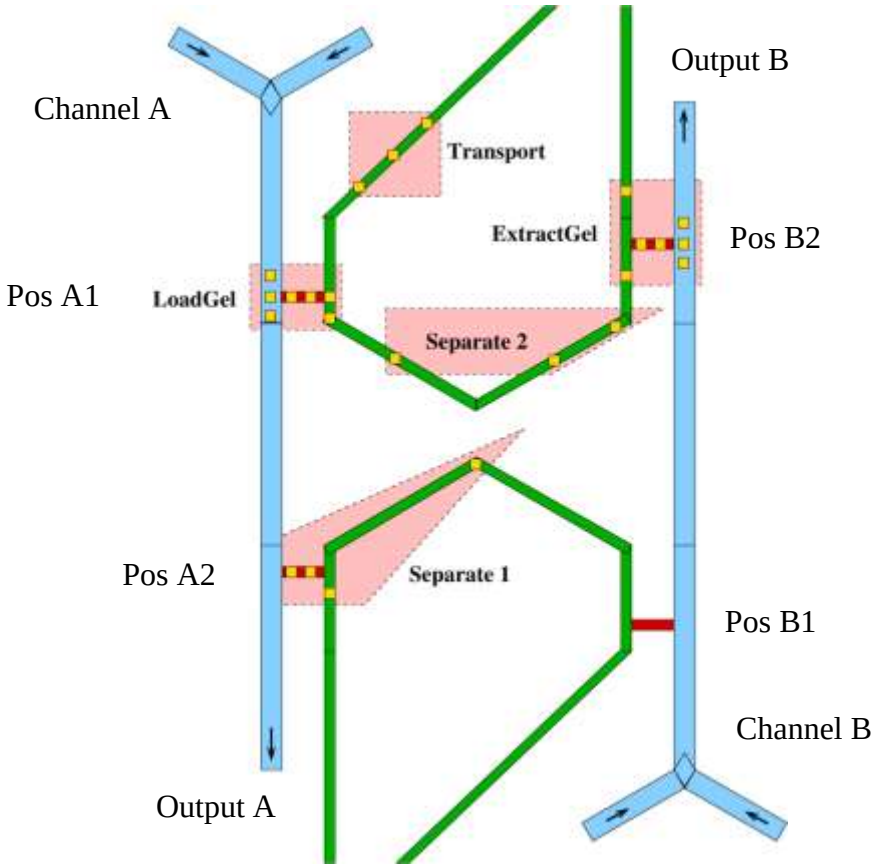


**Figure 5.4.21:** Annotated Figure 1 to allow for a specification of the MATCHIT-IML algorithm.

### Integration

All these operations from MATCHIT-IML are required to specify a higher level on what the whole system is about to do. In Listing 4, a procedure is depicted which creates a droplet (chemtainer X), waits for this chemtainer at position A2, see Figure 5.4.21, extracts the DNA from the chemtainer, separates the DNA in area Separate 1, picks the longer DNA from this separation, transports it to position B1 and injects that into a newly created droplet (chemtainer Y). This chemtainer Y is then moved to position B2, stopped there, and the DNA is extracted again and a second separation done in zone Separate 2, now selecting the shortest DNA-fragments. This shortest DNA-fragement is inserted into a new droplet (chemtainer Z) and transported to the output A.

```
Init{
create droplet channelA X
assign next 0
}

Process {
posA2_droplet: sequence separ1
posA1_droplet and next: sequence separ2
}

Separ1{
stop channel A
extract
start channel A
create droplet channelB Y
separate Separate 1 slowest
transport slowest posB1
posB1_droplet: inject
start channel B
assign next 1
}

Separ2{
stop channel B
extract
start channel B
create droplet channelA Z
separate Separate 1 fastest
transport fastest posA1
posA1_droplet: inject
start channel A
halt
}
```

**Listing 4:** A program in notation of MATCHIT-IML which is already close to a formal description of the problem and as such suited to be coupled with MATCHIT-calculus.

## 6. Summary and conclusions

In this deliverable, we have documented electronic control of a complete set of operations on chemtainers, primarily droplets but also vesicles, that link up processes of reactive chemical synthesis in chemtainers with other operations required for ongoing (e.g. iterative) chemtainer processing. The range of chemical systems studied and presented in Section 2 is diverse, but focuses on elementary rapid reactive processes associated with DNA: DNA ligation, DNA immobilization and DNA hybridization using duplex and triplex interactions. These operations allow specific addressing of chemtainers to specific sites in the matrix (e.g. vesicles, beads and droplets) as well as specific chemtainer-chemtainer interactions either stemming from the former or directly mediated by DNA interactions (e.g. bead-bead interactions of 2.8, or the vesicle-vesicle interactions of WP2). These results are readily extendable to other chemtainers such the DNA tetrahedron investigated in WP1,

which can also be embedded in aqueous droplets. Because of its importance for ongoing chemtainer processing, we have described the implementation of the control flow from high level language to low level software and microfluidic hardware in most detail for the process of chemtainer "cleanup" involving extraction, separation and selective injection. The MATCHIT calculus provides an abstract representation of these processes which is made more explicit in the MATCHIT-IML prior to being mapped to the low level language (biopro). Although much work remains to be done, the deliverable completes the pilot research in MATCHIT establishing and demonstrating the basic operational principles of a computer programmable electronic chemical matrix able to deal with chemistry in a MIMD fashion at the level of DNA-addressed chemtainers.

**Participants and authors:**

**Uwe Tangen*, Abhishek Sharma, Patrick Wagler*, Gabriel A. Minero, Thomas Maeke, and John S. McCaskill***
BioMIP: Microsystems Chemistry and BioIT, Ruhr Universität Bochum, Germany. (RUB)

**Harold Fellermann, Carsten Svaneborg, Martin Hanczyk, Maik Hadorn, Eva Bönzli, Steen Rasmussen**
FLinT Center for Fundamental Living Technology, University of Southern Denmark, Denmark (SDU)

* Main authors.